IEEE Access
Multidisciplinary | Rapid Review | Open Access Journal

Received January 18, 2021, accepted January 25, 2021, date of publication February 4, 2021, date of current version February 16, 2021.

Digital Object Identifier 10.1109/ACCESS.2021.3057242

Dual-Determination of Modulation Types and Signal-to-Noise Ratios Using 2D-ASIQH Features for Next Generation of Wireless Communication Systems

TARIK ADNAN ALMOHAMAD[1], (Member, IEEE), MOHD FADZLI MOHD SALLEH[2], (Member, IEEE), MOHD NAZRI MAHMUD[2], İSMAIL RAKIP KARAŞ[3], NOR SHAHIDA MOHD SHAH[4], (Member, IEEE), AND SAMIR AHMED AL-GAILANI[2,5], (Member, IEEE)

[1]Electrical-Electronics Engineering Department, Faculty of Engineering, Karabük University, 78050 Karabük, Turkey
[2]School of Electrical and Electronic Engineering, Universiti Sains Malaysia, Nibong Tebal 14300, Malaysia
[3]Computer Engineering Department, Karabük University, Demir Celik Campus, 78050 Karabük, Turkey
[4]Faculty of Engineering Technology, Universiti Tun Hussein Onn Malaysia, Pagoh Higher Educational Hub, Johor 84600, Malaysia
[5]Department of Electrical and Electronics Engineering, Al-Madinah International University, Kuala Lumpur 57100, Malaysia

Corresponding authors: Tarik Adnan Almohamad (tam_jami@hotmail.com) and Mohd Fadzli Mohd Salleh (fadzlisalleh@usm.my)

This work was supported in part by the Universiti Sains Malaysia (USM) Fellowship Scheme and in part by the Research University Individual (RUI) grant under Grant 8014051.

ABSTRACT In order to pursue rapid development of the new generation of wireless communication systems and elevate their security and efficiency, this paper proposes a novel scheme for automatic dual determination of modulation types and signal to noise ratios (SNR) for next generations of wireless communication systems, fifth-generation (5G) and beyond. The proposed scheme adopts unique signatures depicted in two-dimensional asynchronously sampled in-phase-quadrature amplitudes' histograms (2D-ASIQHs)-based images and applies the support vector machines (SVMs) tool. Along with the estimation of the instantaneous SNR values over 0-35 dB range, the determination of nine modulation types that belong to different modulation categories i.e., phase-shift keying (Binary-PSK, Quadrature-PSK, and 8-PSK), amplitude-shift keying (2-ASK and 4-ASK) and quadrature-amplitude modulation (4-QAM, 16-QAM, 32-QAM, and 64-QAM) could be achieved by this scheme. The application of this scheme has been simulated using a channel model that is impaired by additive white Gaussian noise (AWGN) and Rayleigh fading, covering a broad range of SNRs of 0-35 dB. The performance of this dual-determination scheme shows high modulation recognition accuracy and low mean SNR estimation error. Therefore, it can be a better alternative for designers of next generation wireless communication systems.

INDEX TERMS Modulation recognition, SNR estimation, 5G communication system, support vector machine, feature-based approach.

I. INTRODUCTION

The recent decades have witnessed a tremendous demand for more secure, reliable, efficient, high-quality and cost-effective wireless and mobile applications and services. Future wireless applications and services are envisaged to lead to a continuous growth of demand for high data rates, quality of service (QoS) and mobility. With the rapid growth of telecommunication systems, it seems that there are many challenges which still cannot be addressed by the current technologies, such as enhancing the QoS of the wireless schemes, securing wireless communication, simplifying implementation complexity, and providing accurate channel state estimation [1]. Automatic determination techniques of signal parameters can be a suitable and potential platform that provides solutions to the abovementioned challenges. In the literature, many techniques for the estimation of signals' parameters, such as modulation type, signal-to-noise

The associate editor coordinating the review of this manuscript and approving it for publication was Md Fazlul Kader.

ratio (SNR), bit-rate, transmitted signal power etc., in wireless communications have been presented [2]–[7].

The transmitters in the next generation wireless networks are expected to vary and adjust some of these parameters based on the existing channel conditions. This, in turn, will demand the receivers that engaged in these systems to be fully equipped with the autonomous determination techniques of various signal parameters. The majority of the existing schemes in the literature focus on identifying one signal parameter for e.g. modulation type i.e. automatic modulation recognition (AMR) [8]–[16] or signal-to-noise ratio (SNR) [17]–[20] rather than on dual identification of multiple parameters. Additionally, they entail tight-synchronous and fast sampling of the detected signals. Besides, the majority of existing AMR or SNR estimation techniques consider only AWGN and not multipath fading channels. This affects vitally on the performance of these present techniques.

In general, signal parameter determination techniques are usually categorized into feature-based (FB) and likelihood ratio-based (LB) approaches [2], [21]. The former scheme exploits the statistical characteristics of the received signals and determines the desired signal parameters based on the extracted features of these characteristics. On the other hand, the latter adopts multiple hypothesis-based solutions, calculates the values of the likelihood functions and compares them with a threshold value in order to make final decisions as elaborated in [22]–[24]. Alternatively, there are few existing techniques adopted in the literature which propose a fusion model of both FB and LB schemes together for modulation formats classification [25], [26]. LB schemes may offer an optimal solution in the determination process but they undergo very high computational complexity [21], [27].

The signal identification, by FB algorithms, is made based on the extraction of single or multiple statistical features from the received signal. For instance, high order cumulants (HOCs) features are used in [28] and in [29], [30] in order to discern the modulation types. However, one drawback of HOCs is that it requires huge number of samples [31]. Besides, poor performance results for higher order QAM modulation as shown in [29], [30]. The average instantaneous amplitude values in conjunction with the maximum value of spectral power density are utilized in [32] for the recognition of modulation types. However, the presented algorithm in [29] outperforms the method in [32] due to its robustness to the noise. In [33], the authors propose a cumulant-based technique to identify only PSK and QAM-based signals with the assumption of having a perfect channel information.

Identification of PSK and QAM signals have been investigated in [16], [27], [34], [35]. The work in [16] focused on the modulation classification of only three types of signals (i.e., QPSK, 16QAM and 64QAM). In the process of modulation identification, they had to apply Cepstrum technique to resist the multipath fading phenomenon. In term of modulation recognition accuracy, their method approached an average value of 80%. The scheme presented in [27] can be concluded as follows: 1) It identifies only four types of modulations (i.e., BPSK, QPSK, 16-QAM and 64-QAM), 2) the scheme applies to a cooperative relay network that requires at least two time slots to perform successful AMR, 3) the communication channel between transmitter and receiver is impaired by flat fading, 4) the modulation recognition accuracies of SVM are quite good, it reaches 98.25% at best (assuming a perfect channel state knowledge), for a pool of signals with four modulations only, 5) the performance of the algorithm depends on intermediate nodes (relays) between source and destination. An outage or any disconnection in these nodes will cause a failure in the entire communication system, 6) the scheme assumes that SNR is known. A Similar modulation family to [27], has been deemed in the work [35] to handle AMR problem using their features-based technique. In their method, authors proposed Bhattacharrya Distance based Feature Selection (BDFS) algorithm and neural network tool to extract distinctive features and differentiate modulations from a set of signals (BPSK, QPSK, 8-PSK, 16QAM). On the other hand, a larger pool of digital signals has been considered in our work, aiming to accurately estimate both the modulation type and the SNR parameters, simultaneously.

A wider range of modulations has been earlier identified in [10] compared to [27]. The modulation candidates to be recognized were FSK, ASK, PSK and QAM-based signals. The analysis in their work was conducted over a specific range of SNR (-4, 0, 4 and 8 dB). The channel effect was limited to Gaussian noise only and the accomplished accuracy was 97.74%. However, they have considered an ideal channel and needed to employ a combination of three types of features for AMR target, that are, i) the instantaneous characteristics, ii) higher order moments (HOMs), and iii) higher order cumulants, which inherently increased the computational complexity. Furthermore, SNR parameter was assumed to be known to the receiver.

Similarly, the work in [36] proposed a solution for AMR problem and utilized SVM tool to recognize a set of modulation types (i.e., FSK, MSK, ASK, PSK and QAM based signals). The proposed solution attained around 97% modulation recognition accuracy. Their model had to extract multiple features from the received signal in order to facilitate the recognition process at the SVM classifier. Moreover, their work was limited to only AWGN, and the SNR parameter assumed to be known.

Another work in [37] utilized graph-based analysis to differentiate between only QAM signals. Their model constructed the graphs based on the cyclic spectra of the detected signal and extracted the features from the corresponding adjacency matrices. Their work attained a modulation recognition accuracy more than 85 %. However, their work considered on only AWGN channel. Moreover, the modulation pool in their model was limited to QAM signals and their classifier was unable to recognize, for example, PSK types due to the fact that QAM and PSK signals have identical cyclic spectra (i.e., same features).

A larger modulation pool was examined in [38] for modulation type recognition using four types of classifiers (i.e., CNN, random forest, extreme gradient boosting trees, and decision tree). They proposed a feature-based model, that is sensitive to the spectrum dynamics of the detected signal, called dyadic aggregated autoregressive model (DASAR) to extract the detected signal features using 200 samples of the signal (i.e., smaller size of dataset). Their technique showed that random forest (RF) classifier performed best with DASAR where and attained average accuracy achieved up to 70.96% at SNR value higher than 10 dB. In addition, observing the performance of the RF classifier in their simulation, there was a difficulty\confusion in differentiating QPSK, 8PSK, and 16QAM from 64QAM signal.

In contrast to [38], a better performance of modulation recognition has been achieved in [39] via convolutional neural network (CNN) tool but considering 1024 samples per transmitted signal (i.e., larger size of dataset compared to [38]). Their model processed analog and digital modulation types under Rayleigh fading channel and obtained an average recognition accuracy of 91.48% at SNR value of 10 dB.

In [34], their proposed algorithm required high values of SNR in order to achieve satisfactory performance. Their technique necessitated an equalizer to tackle the effect of multipath fading.

Wavelet transform-based features were also utilized for the discrimination of digital modulation types in the literature [40], [41]. One drawback of these proposed recognition methods is that, with only AWGN channel, they were unable to recognize advanced modulation schemes such as QAM signals. In that respect, the techniques applied in the aforementioned work performed identification of only one signal parameter i.e., modulation type, and overlooked the instantaneous SNR values or assumed the knowledge of SNR is known.

Alternative types of features are the spectral instantaneous amplitude, phase and frequency were used in combination with cumulant in [42] in order to distinguish between PSK and QAM signals. The channel impairments were the frequency selective fading. The achievable accuracy was 93.21%. In their work, they assumed that the carrier frequency is known at the receiver as they assumed the signal to be already in baseband form. In addition, their algorithm was unable to estimate the channel quality i.e. SNR and instead the SNR knowledge was assumed to be perfectly known at the receiver. Moreover, learning machine DNN was used. Its training process occurred deeply among all layers and nodes where all had to connect with each other to perform the deep learning process, which in turn increased the computational complexity especially when the training dataset is small. DNN usually requires large input data which is impractical when small training dataset is considered.

Recently we have proposed the 2D-ASIQHs-based model in [43]. The proposed feature-based approach in that work was examined to recognize a single parameter (modulation) i.e., four digital modulation types and the channel is limited to AWGN only. In the presented work of this paper, we have extended our work in [43] and investigated the proposed model for multiple signal parameters with larger pool of modulation types and wide range of SNRs under realistic environment (i.e., multipath fading channel).

On the other hand, an estimation technique of SNR was proposed in [44]. In their work, frozen bits of polar codes-based features were adopted to assist for SNR estimation. The mean error of SNR estimation was calculated over a short range of SNR values (i.e., 0–5 dB). The estimation result of SNR obtained according to the mapping of the SNR values to the frozen bit error rate. These features were able to provide the receiver only SNR information but were not capable of modulation type recognition which is an essential knowledge for data recovery. Furthermore, the channel considered was a simple communication medium (i.e., AWGN channel).

Very few techniques for simultaneous determination of several signal parameters have been suggested recently such as the asynchronous amplitude histograms (AAHs)-based techniques in [45] and the asynchronous delay-tap plots (ADTPs)-based techniques in [7], [46]. The researchers who proposed these schemes conducted their experiments to classify three modulation types (2ASK, QPSK and 16QAM). One limitation of these techniques is that they are incapable of identifying more than one type of PSK signals. This is due to the fact that, based on their proposed features, PSK signals would have identical patterns as all PSK types are characterized with only one unique amplitude.

Moreover, the work in [46] is limited to only AWGN channel before it is extended in [7] for fading channel. Additionally, its implementation necessitates an extra sampler to acquire the samples of the envelope signal which in turn will lead to more installed hardware components in the non-coherent receiver. Besides, it requires a delay in time Δt between the two samplers employed in their technique in order to construct their features. Furthermore, the data rates of the modulated signals are associated with the tap-delay between both samplers, hence further adjustment is demanded accordingly which subsequently raises the implementation complexity [47].

Unlike their works, the presented scheme in this paper devotes the existing hardware structure in coherent receiver to establish the proposed 2D asynchronous In-phase-Quadrature histograms (2D-ASIQHs)-based images where no additional hardware devices are required. It offers a more generic receiver that can simultaneously determine any of the nine modulation types (including 3 types of PSK modulation family) and the instantaneous SNRs, under AWGN and Rayleigh fading channels.

Recently, many researchers deploying machine learning tools and their applications in their automatic signal recognition methods which also cover paradigms in future 5G wireless networks [48], [49]. It morphs to be a trend in the field due to the significant capabilities they provide. Such tools are artificial neural network (ANN) [11], [50]–[52],

deep\ convolutional neural network (DNN\CNN) [53]–[59] and support vector machine (SVM) [9], [45], [60]–[62].

SVM technique has proven its superiority in a vast range of real-world problems [63] in term of classification [64] and regression [65] as well as in avoiding overfitting problem [48], [61], [66]. Moreover, according to the comparative study and experiments conducted by authors in [67], SVM was more flexible than sparse auto-encoder (SAE) in dealing with datasets that are characterized by small size of training samples. Hence, SVM is adopted in this presented scheme.

In fact, automatic simultaneous determination of multiple signal parameters (such as modulation types, transmitted powers, data rates, SNRs and so on) in wireless communications systems still lack of investigation and not widely addressed. Therefore, in this paper, we propose one sole technique that can identify simultaneously several parameters i.e., modulation types and SNRs. Furthermore, as FB algorithms provide a near-optimal solution with less computational complexity in contrast to LB hence, this approach is adopted in this paper. The contributions of the proposed work lie in the following folds:

- The proposed mechanism enables a reliable automatic dual-determination of nine different modulation types and wide range of SNRs in the coherent receivers. The simultaneous determination process of the aforementioned parameters exploits only one algorithm to achieve its goal unlike most of the up-to-date methods which employ more than one algorithm to determine the two parameters individually.
- The proposed scheme simplifies the sampling process by utilizing low speed and asynchronous sampling to produce patterns based on novel statistical features called (2D-ASIQHs) which reveal unique signatures among various wireless modulated signals. The proposed algorithm requires no synchronous sampling process; i.e., does not necessitate sampling at the center (peak) of the symbol period (requiring no tight synchronization and timing knowledge between source and destination) hence less hardware and computational complexity.
- The scheme offers significant determination accuracies and robust resistance against the existence of both AWGN and real-world scenarios (Rayleigh fading channels). This has been achieved through utilizing a combination of statistical features and SVM tool for the simultaneous automatic determination of modulation formats and SNRs. Furthermore, the algorithm produces unique signatures of each modulation types even in faded channels, making equalizer unnecessary for tackling the effect of fading.
- The presented model persistently aims to diminish the implementation complexity by decreasing the number of generated ASIQHs features. The reduction in features' size is performed by employing principal component analysis (PCA) method to extract the most important features of (2D-ASIQHs)-based images before input them to the SVMs tool.

The remainder of this manuscript is outlined as follows. Section II illustrates the concept of the proposed features. Section III explains the system model. Section IV manifests the operating mechanism. Section V demonstrates the simulation results and finally Section VI concludes the entire framework.

II. CONCEPT OF TWO-DIMENSIONAL ASYNCHRONOUS IN-PHASE-QUADRATURE HISTOGRAMS (2D-ASIQHS)

In this paper, new asynchronous sampling-based images which reflect statistical features are proposed. These images are made of two dimensional histograms that were constructed by asynchronously sampling the In-phase-Quadrature components and then calculating the occurrences of their captured samples. The 2D-ASIQHs images reveal distinct signatures of digitally modulated signals. The presented ASIQHs-based technique offers cost-effectiveness, flexibility, and simplicity in its implementation as it exploits the existing structure of the coherent receiver without any costly modifications. Fig. 1 illustrates the concept of generating 2D-ASIQHs-based images.

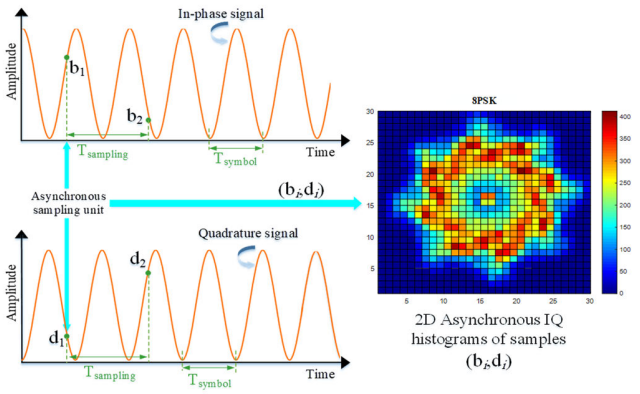

FIGURE 1. Fundamental of 2D-ASIQHs by utilizing asynchronous-IQ signals sampling. T_{symbol} & $T_{sampling}$ refer to symbol period and sampling period respectively.

The stages of generating 2D-ASIQHs-based images can be summarized as follows: foremost, the in-phase-quadrature components captured from a detected signal are arbitrarily sampled by a low-speed asynchronous sampling unit at a lower value of sampling rate than its symbol rate. It is worth to mention here that the sampling rate value is uncorrelated with the symbol rate. More specifically, the symbol period T_{symbol} is much shorter than the sampling period $T_{sampling}$. Next, the samples $S_i = \{b_i, d_i\} \in S = \{S_i | i = 1, 2, \ldots, N\}$ are ranked based on their voltage magnitude values. Mathematically, S_i can be represented as a group of two values $S_i = \{b_i, d_i\}$ or in the complex domain $S_i = b_i + jd_i$. Let's consider a 2D plane consists of $M \times M$ of arrays of bins. Then, each sample S_i is mapped into its corresponding bin's subgroups

as shown in (1):

$$\boldsymbol{S}^{(r,c)} = \{S_i | S_i \in V_{r,c}, i = 1, 2, \ldots, N\} \tag{1}$$

where N is the number of samples, r and c denote rows and columns indices respectively, and $V_{r,c}$ denotes the complex sub-range of the bin located at (r, c) in the 2D-plane as shown in (2) below:

$$V = \begin{bmatrix} V_{0,0} & V_{0,1} & \cdots & V_{0,M-1} \\ V_{1,0} & V_{1,1} & \cdots & V_{1,M-1} \\ \vdots & \vdots & \vdots & \vdots \\ V_{M-1,0} & V_{M-1,1} & \cdots & V_{M-1,M-1} \end{bmatrix} \tag{2}$$

The bins' subgroups $\mathbf{S}^{(r,c)} \subset S, \mathbf{S}^{(r,c)} \in V_{r,c}$ can be easily assembled by simply processing the real and imaginary components of the samples S_i separately as follows:

$$\Re\left(\boldsymbol{S}^{(r,c)}\right) = \left\{\Re\left(S_i\right) | \Re\left(S_i\right) \in \Re\left(V_{0,c}\right), i = 1, 2, \ldots, N\right\} \tag{3}$$

$$\Im\left(\boldsymbol{S}^{(r,c)}\right) = \left\{\Im\left(S_i\right) | \Im\left(S_i\right) \in \Im(V_{r,0}), i = 1, 2, \ldots, N\right\} \tag{4}$$

where $\Re(V_{0,c})$ and $\Im\left(V_{r,0}\right)$ are the real and imaginary components of the c^{th} and r^{th} sub-range of $V_{r,c}$ respectively and they are defined as follows:

$$\begin{aligned} \Re\left(V_{0,c}\right) &\subset \left[\left[V_{LOW}^{I} V_{1}^{I}\right], \left(V_{1}^{I} V_{2}^{I}\right], \ldots, \left(V_{M-1}^{I} V_{HIGH}^{I}\right]\right] \\ &= \begin{cases} (V_{c}^{I} V_{c+1}^{I}], & c > 0 \\ [V_{LOW}^{I} V_{1}^{I}], & c = 0 \end{cases} \end{aligned} \tag{5}$$

$$\begin{aligned} \Im\left(V_{r,0}\right) &\subset \left[\left[V_{LOW}^{Q} V_{1}^{Q}\right], \left(V_{1}^{Q} V_{2}^{Q}\right], \ldots, \left(V_{M-1}^{Q} V_{HIGH}^{Q}\right]\right] \\ &= \begin{cases} (V_{r}^{Q} V_{r+1}^{Q}], & r > 0 \\ [V_{LOW}^{Q} V_{1}^{Q}], & r = 0 \end{cases} \end{aligned} \tag{6}$$

where $\left[V_{\mathrm{LOW}}^{I} V_{\mathrm{HIGH}}^{I}\right]$ and $\left[V_{\mathrm{LOW}}^{Q} V_{\mathrm{HIGH}}^{Q}\right]$ are the samples' full ranges of real and imaginary components respectively, that is: $\Re\left(S_i\right) \in \left[V_{LOW}^{I} V_{HIGH}^{I}\right]$ and $\Im\left(S_i\right) \in \left[V_{LOW}^{Q} V_{HIGH}^{Q}\right]$.

On the other hand, the sub-ranges component V_m is given by:

$$V_{m}^{I} = V_{LOW}^{I} + \frac{m\left(V_{HIGH}^{I} - V_{LOW}^{I}\right)}{M} \tag{7}$$

$$V_{m}^{Q} = V_{LOW}^{Q} + \frac{m\left(V_{HIGH}^{Q} - V_{LOW}^{Q}\right)}{M} \tag{8}$$

Finally, the total number of occurrences of the amplitude samples that lie within each of the bins' range is calculated for 2D plane as

$$\mathcal{N} = \begin{bmatrix} \mathrm{n}\left(\mathbf{S}^{(0,0)}\right) & \mathrm{n}\left(\mathbf{S}^{(0,1)}\right) & \cdots & \mathrm{n}\left(\mathbf{S}^{(0,M-1)}\right) \\ \mathrm{n}\left(\mathbf{S}^{(1,0)}\right) & \mathrm{n}\left(\mathbf{S}^{(1,1)}\right) & \cdots & \mathrm{n}\left(\mathbf{S}^{(1,M-1)}\right) \\ \vdots & \vdots & \vdots & \vdots \\ \mathrm{n}\left(\mathbf{S}^{(M-1,0)}\right) & \mathrm{n}\left(\mathbf{S}^{(M-1,1)}\right) & \cdots & \mathrm{n}\left(\mathbf{S}^{(M-1,M-1)}\right) \end{bmatrix} \tag{9}$$

where $\mathcal{N}$ represents the number of occurrences matrix and $\mathrm{n}\left(\mathbf{S}^{(r,c)}\right)$ denotes the number of elements/samples in the subgroup $\mathbf{S}^{(r,c)}$. Eventually, by pinning the number of occurrences on two dimensional plane, the 2D-ASIQHs images are produced, where the value of each bin will create another dimension that can be represented as colour.

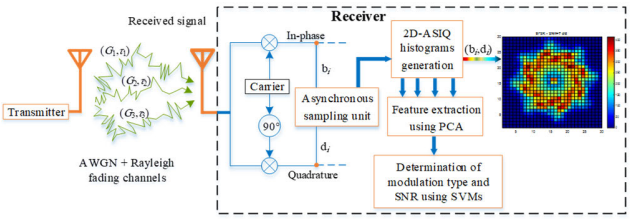

FIGURE 2. System model employed in the simulations.

III. SYSTEM MODEL

Figure 2 illustrates the system model and the parameters utilized in this model are presented in Table 1.

TABLE 1. Values of Parameters Used in the Simulations

Quantities	Values
symbol rate	250×10^6 symbols/s
carrier frequency	2.5 GHz i.e. 10 times of the symbol rate used
sampling rate	15 Mbps
symbol period	$1/(250 \times 10^6) = 4 \times 10^{-9}$s
pulse shaper	Raised-cosine pulse shaping filter used with Roll-off factor $R_\alpha = 0.75$
modulation types	BPSK, 2-ASK, QPSK, 4-ASK, 8-PSK, 4-QAM, 16-QAM, 32-QAM, 64-QAM
SNRs	0–35 dB with a step of 0.5 dB
channel type	AWGN and Rayleigh fading channels
three path gains G_i and delays τ_i	Uniformly distributed in the range of -20–0 dB and 0–1 μs, respectively.
machine learning	Support vector machine (SVM)
No. of observations	6390
total No. of features	900 (before reduction algorithm)

The values given in Table 1 present different parameters employed in the simulations. The transmission rate of symbols and the carrier frequency are 250×10^6 symbols per second and 2.5 GHz respectively, assuming that the carrier frequency is known at the receiver. The Raised-cosine pulse shaper is utilized for shaping the considered signals which are impaired by AWGN and three-path Rayleigh fading channels. Rayleigh fading parameters are set to be varied where all paths' gains G_i and delays τ_i are randomly altered and uniformly distributed in the ranges of -200 dB and $0-1\mu s$, respectively.

The delay for each path between transmitter and receiver is given as follows

$$\tau_i = T_{\mathrm{LoS}} + \alpha_i T_{\mathrm{s}} \tag{10}$$

where $i \in \{1, 2, 3\}$, T_{LoS} is the delay of the direct path, T_{s} is the symbol period and α_i is uniformly distributed random variable in the range between 0 and 0.5.

A coherent receiver-based detection is executed at the receiver side where the detected signal is multiplied by a carrier signal to obtain the in-phase and quadrature components. Subsequently, the resultant components are asynchronously sampled both simultaneously at a sampling rate lower than a symbol rate. The term ''asynchronously'' here means that the sampling process is not necessarily to be at the center of the symbol period, that is, the receiver does not require a tight-synchronization\timing algorithm to detect the peaks' centers of the symbols. This reduces the hardware implementation complexity, cost and increases the speed of constructing the features. A total of 110,000 sample pairs (b_i, d_i) are acquired to be utilized afterwards to construct the 2D-ASIQ histograms with dimensions 30 × 30 bins of each image.

In order to decrease the computational complexity of the presented mechanism, an extraction of most significant 2D-ASIQHs features is performed through the execution of the PCA algorithm. Next, the extracted features are fed to the SVMs for the training process in order to generate the trained SVM model. In order to investigate the signal parameters-determination capabilities of the proposed mechanism, nine formats of diverse modulation types which are descended from different grades of amplitudes and phases based modulations, are adopted to form the pool of modulation classes (BPSK, 2-ASK, QPSK, 4-ASK, 8-PSK, 4-QAM, 16-QAM, 32-QAM, 64-QAM).

Multipath fading phenomena usually describe the statistical changes in the received signal which arrives at the receiver through multiple spreading paths P_{i} with various path gains G_i and delays τ_i. Let $m(\mathrm{t})$ is the baseband signal, the equivalent transmitting passband signal is described as follows [68]:

$$\tilde{m}(\mathrm{t}) = Re[m(\mathrm{t})e^{2j\pi f_c t}] \tag{11}$$

where $Re\,[.]$ is the real component of the modulated signal. Given the signal will arrive at the receiver over a fading channel with three propagation paths P_{i}, the detected passband signal can be given as

$$\begin{aligned}\tilde{x}\,(\mathrm{t}) &= Re\left[\sum_{i=1}^{P_i=3} G_i e^{2j\pi f_c(t-\tau_i)} m\,(t-\tau_i)\right] \\ &= Re\left[x_s(t)e^{2j\pi f_c t}\right]\end{aligned} \tag{12}$$

where G_i, f_c and τ_i refer to the path gain (dB), carrier frequency (Hz) and path delay respectively, while the baseband signal $x_s(t)$ is described as

$$x_s(\mathrm{t}) = \sum_{i=1}^{P_i=3} G_i e^{-j\emptyset_i(t)} m\,(t-\tau_i) \tag{13}$$

where $\emptyset_i\,(t) = 2\pi f_c \tau_i$. Based on (13), the corresponding channel can be represented as liner time-varying filter, and the impulse response of the channel is given by

$$h\,(t,\tau) = \sum_{i=1}^{P_i=3} G_i e^{-j\emptyset_i(t)} \delta\,(t-\tau_i) \tag{14}$$

where $\delta(\cdot)$ is the Dirac delta function. Equation (14) can be modelled and described as

$$h\,(t,\tau) = h\,(t)\,\delta\,(t-\tau_i) \tag{15}$$

where $h\,(t) = \sum_{i=1}^{P_i=3} G_i e^{-j\emptyset_i(t)}$. The detected passband $\tilde{x}\,(\mathrm{t})$ signal can be represented as follows:

$$\begin{aligned}\tilde{x}\,(\mathrm{t}) &= Re\left[x_s\,(t)\,e^{2j\pi f_c t}\right] \\ &= Re\left[\left\{h_I\,(t) + jh_Q\,(t)\right\} e^{2j\pi f_c t}\right] \\ &= h_I\,(t)\,cos2\pi f_c t - h_Q\,(t)\,sin2\pi f_c t\end{aligned} \tag{16}$$

where $h_I\,(t)$ is the in-phase component given in (17), and $h_Q\,(t)$ is the quadrature component expressed in (18)

$$h_I\,(t) = \sum_{i=1}^{P_i=3} G_i cos\emptyset_i\,(t) \tag{17}$$

$$h_Q\,(t) = \sum_{i=1}^{P_i=3} G_i sin\emptyset_i\,(t) \tag{18}$$

By simultaneously performing an asynchronous sampling of the signals represented by (17) and (18), the 2D-ASIQ histograms are thus constructed.

Figure 3 portrays an example of 2D-ASIQHs for the nine modulation types considered in the presented scheme at two different values of SNRs. From the figure, it can be evidently observed that the features, reflected in the two-dimensional histograms (i.e., image) pertaining to various modulation types, SNRs, different path gains and delays, produce unique signatures. This uniqueness enables accurate signal parameters recognition. Besides, the patterns in 2D-ASIQHs images also vary when the SNR values are changed. It can be observed that these proposed features are sensitive to the variations of modulation type, SNR, path gains and delays all at the same time. Hence, these features enable a simultaneous determination of modulation types and SNRs with the employment of SVMs.

IV. THE OPERATING MECHANISM

These 2D-ASIQHs images reflect distinctive features that subsequently can be exploited for joint determination of modulation types and SNRs. This dual determination of the aforementioned parameters can be achieved through an automated system based on machine learning techniques such as SVMs. In the presented mechanism, two different SVMs are utilized, namely support vector classifier (SVC) to determine the modulation type and support vector regressor (SVR) to determine the signal's quality measures (i.e., SNRs).

A large dataset $\{\ddot{\mathrm{X}}_{ASIQH}, \ddot{\mathrm{E}}_{ASIQH}\}$ is constructed from 6390 ASIQHs correspond to permutations of 9 types of wireless signals, 71 SNRs and 10 random alterations of

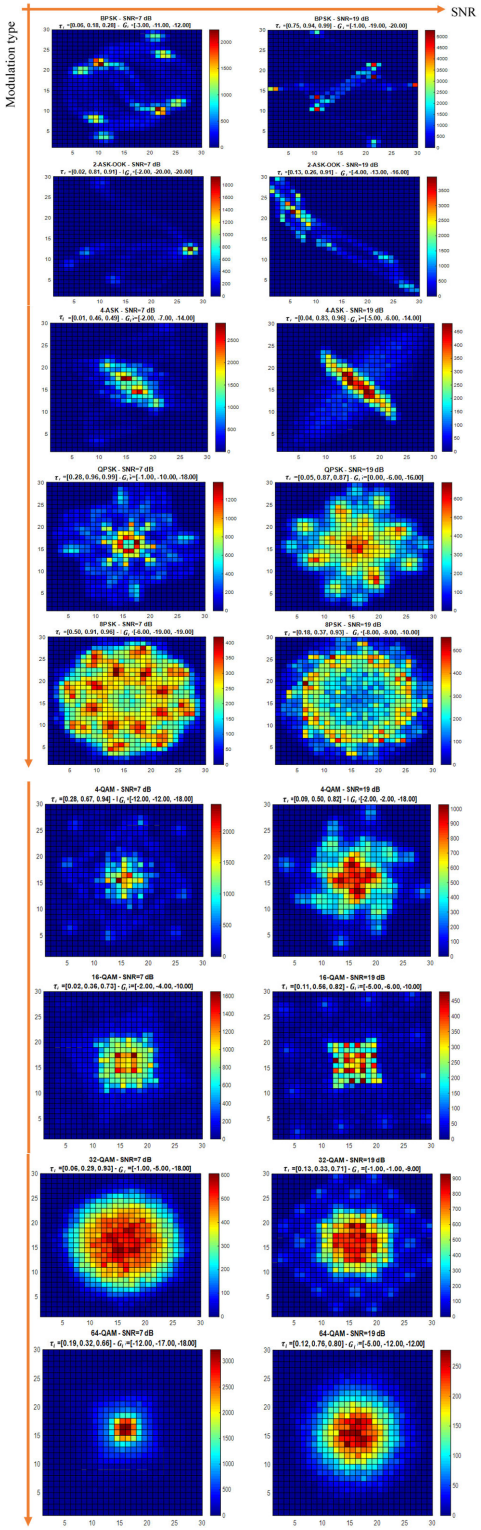

FIGURE 3. 2D-ASIQHs for various modulation types, different SNRs, path gains and delays. The first column illustrates ASIQHs at SNR=7dB, and the second column portrays ASIQHs at SNR= 19 dB, where τ_i is the path delay and G_i is the path gain.

channel gains and delays that is, $6390 = 9 \times 71 \times 10$. The constructed dataset is split into training and testing sub-sets by using 5-folds cross-validation technique.

The 5-fold cross validation method splits randomly the entire 2D-ASIQHs dataset (i.e., 6390 observations\samples) into five subsets with equal size. Then four subsets (i.e., 5112 observations) are exploited for the training stage of SVM whereas one subset (i.e., 1278 observations) of total 2D-ASIQHs is employed for the testing stage. This procedure is repeated five times (the recognition accuracies are calculated every time) and finally the average recognition accuracy is calculated by taking the mean of all accuracies in the entire five rounds. The recognition accuracy is given as

$$A_{ci} = \frac{C_s}{E_s} \times 100\% \tag{19}$$

where E_s is the size of entire testing data set and C_s is the number of successfully determined samples. It is worth to mention that in the training phase, a 5-fold cross validation method is also carried out over the training subset (4 subsets for training and 1 subset for validation) in order to produce the optimized-trained model [69].

A. FEATURES EXTRACTION VIA PRINCIPAL COMPONENTS ANALYSIS

One target of the proposed scheme is to diminish the processing complexity. This is attained by decreasing the number of generated ASIQHs features and extract the most useful ones without losing additional considerable data. The reduction of features' size in this work is performed by engaging a well-known technique namely the principal component analysis (PCA) method. Recently, PCA has gained a notable interest as a beneficial strategy in representing a dataset in a new form and reducing the size of features. It finds applications in many research areas such as learning algorithms, patterns recognition and feature extraction [70]–[72]. It drastically decreases the dataset dimensionality and extracts the most important features of (2D-ASIQHs)-based images with preserving the data distribution. The new reduced-dimensional subspace contains uncorrelated and descriptive variables what so-called principal components (PCs). These PCs are then ranked in descending order based on their highest to the lowest variance values before inputting them to the SVMs tool. The PCs can be efficiently obtained by calculating the eigenvectors of the dataset. The steps towards the implementation of PCA algorithm can be summarized as follows

1. Assume a matrix $\ddot{\mathrm{X}}$ represents a training subset, has S ASIQHs-images. Let every ASIQHs-image has a size of $V \times V$ (i.e., 30×30 pixels).
2. The ASIQHs-images can be handled as vectors by performing a concatenation process on the rows (or columns) of these images before input them to SVM. Hence, it can be described as a one-dimensional vector x_i of length V^2.Therefore, the large matrix $\ddot{\mathrm{X}}$ of size $V^2 \times S$ is established where $\ddot{\mathrm{X}} = [x_1, x_2, \ldots, x_S]$. Each 2D-ASIQH in the dataset is represented by a $V^2 \times 1$ vector x_i.

3. Calculate the mean ASIQHs vector γ of matrix $\ddot{\mathrm{X}}$ by:

$$\gamma = \frac{1}{S}\sum_{i=1}^{S} x_i \tag{20}$$

4. Calculate the zero mean matrix Z by subtracting the mean vector γ from every column in $\ddot{\mathrm{X}}$, we obtain $Z = [z_1, z_2, \ldots, z_S]$ where $z_i = x_i - \gamma$.
5. Obtain the covariance matrix C of Z with size $V^2 \times V^2$ as

$$C = \frac{1}{S}\sum_{i=1}^{S} z_i z_i^T = \frac{1}{S} Z * Z^T \tag{21}$$

where C is diagonalizable matrix (i.e., symmetric).
6. Calculate the eigenvectors and eigenvalues: The covariance matrix C possess V^2 eigenvectors (p_i) and eigenvalues (ξ_i). Next, the principal components (PCs) i.e., eigenvectors p_i, can be determined by solving (22):

$$Cp_i = \xi_i p_i, \quad i = 1, 2, \ldots, V^2 \tag{22}$$

7. Sort the eigenvectors p_i in a descending rank based on their corresponding eigenvalues ξ_i (i.e., variances)
8. Select the desired quantity of PCs having highly-ranked variances: chosen number ($R \ll V^2$) of the sorted eigenvectors is decided. The decision of R is made that the following condition is fulfilled:

$$\nabla = \sum_{i=1}^{R} \xi_i / \sum_{i=1}^{V^2} \xi_i > M_c \tag{23}$$

where typical value of M_c is chosen to be larger than 0.9 [72], [73]. The selected PCs construct R–dimensional eigenspace, which is a subset of the original V^2–dimensional space of matrix $\ddot{\mathrm{X}}$.
9. In this subspace, a weighted-sum of the chosen eigenvectors can approximate any vector z_i as:

$$z_i \approx \sum_{r=1}^{R} h_r p_r \Longrightarrow h_r = p_r^T z_i, \quad r = 1, 2, \ldots, R \tag{24}$$

The feature vector H_T of the ASIQHs-image is comprised of weights h_r, where $H_T = [h_1, h_2, \ldots, h_R]^T$. Based on (24), feature vectors for all ASIQHs images can be calculated for the training subset.
10. To obtain the feature vectors for the testing subset, assume a matrix $\ddot{\mathrm{X}}_E$ has S_E ASIQHs-images with size of $V \times V$ for each observation. Similar to step 1, we obtain matrix $\ddot{\mathrm{X}}_E$ of size $V^2 \times S_E$ where $\ddot{\mathrm{X}}_E = \left[x_{E1}, x_{E2}, \ldots, x_{S_e}\right]$.
11. As in online identification process, only one observation (i.e., one ASIQHs image) will instantly be detected at the receiver, therefore, the mean ASIQHs vector γ obtained in step 3 using (20) will be used to calculate the zero mean matrix Z_E for the testing subset, therefore, $Z_E = [z_{E1}, z_{E2}, \ldots, z_{S_e}]$, $z_{Ei} \in Z_E$, where $z_{Ei} = x_{Ei} - \gamma$.

Finally, the weights h_r of the feature vector H_E can be derived as:

$$h_r = p_r^T z_{Ei} \tag{25}$$

The symbol H will hereafter denote a feature vector in general, which will be used as an input to the machine learning tool.

On the other hand, for every ASIQHs in the training and testing subsets, we generated a 9×1 label vector e and a scalar target e‘. The label vector e will be compared with the SVM output vector containing eight ‘-1’ elements and a single ‘+1’ element whose location signifies the actual modulation type pertains to that ASIQHs. The scalar target e‘ represents the actual SNR target pertaining to that ASIQHs too.

The outputs O and O‘ are anticipated to resemble the corresponding label e and the actual value e‘ respectively. As the supervised learning manner of the machine learning technique is adopted here, both SVC and SVR are trained by employing vector H as input while label e (with size of 9×1) and scalar e‘ as *actual* targets depicted in Fig. 4.

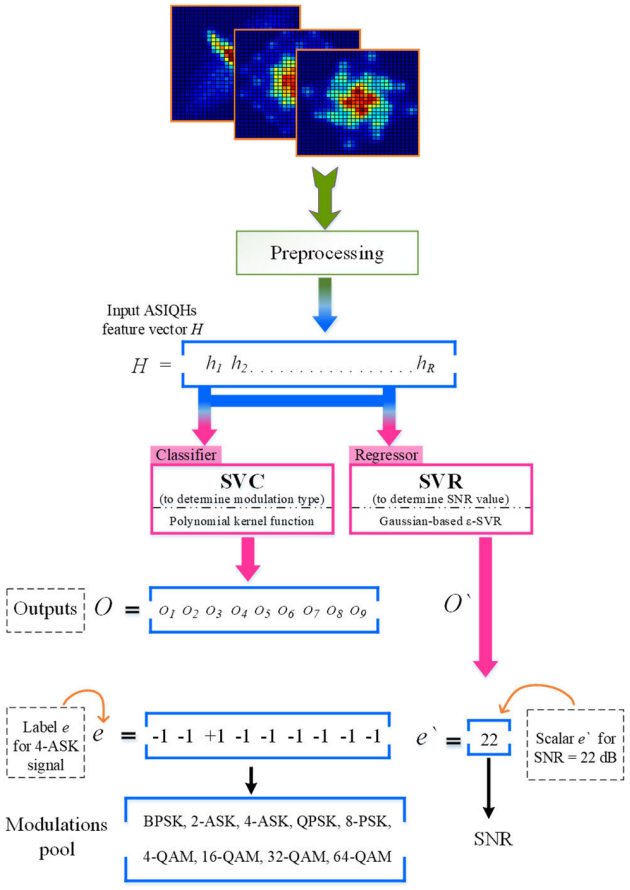

FIGURE 4. SVC and SVR with ASIQHs vector H as input and identified modulation type and estimated SNR as outputs. O is the output vector which holds a single ‘+1’ element and ‘−1s’ elsewhere.

In the presented scheme, one-against-all-based SVM approach is adopted which is a common strategy in handling

TABLE 2. Recognition Accuracies for Different Modulation Types by Employing the Proposed Mechanism (for AWGN and Rayleigh Fading Channel)

Actual modulation types	Recognized modulation types								
	BPSK	2-ASK	4-ASK	QPSK	8-PSK	4-QAM	16-QAM	32-QAM	64-QAM
BPSK	**99.33**	0	0	0	0	0	0.27	0.27	0.13
2-ASK	0	**99.97**	0	0	0	0	0.03	0	0
4-ASK	0	0	**99.97**	0	0	0	0	0.03	0
QPSK	0	0	0	**97.98**	0.17	0.06	0.55	1.12	0.12
8-PSK	0	0	0	0	**98.99**	0	0.36	0.61	0.04
4-QAM	0	0	0	0.20	0.17	**96.90**	1.55	0.76	0.42
16-QAM	0	0	0	0	0.06	0	**99.27**	0.39	0.28
32-QAM	0	0	0	0	0.40	0	0.15	**99.39**	0.06
64-QAM	0	0	0	0	0	0	0.23	0	**99.77**

multi-class SVMs to generate the SVC models. In this approach, a polynomial kernel function is used to assist every SVC to discern a modulation type ('+1') from the remaining classes ('-1s') in the training phase. This function will map the training observations to a higher dimensional space and optimize a hyperplane that maximally separates up observations (i.e., training samples) of each class from the residual types.

Furthermore, in order to fulfill the simultaneous determination, the proposed mechanism also offers, besides modulation recognition, to simultaneously estimate the SNR value by employing Gaussian-based SVR. The goal is to acquire a function that diverges from the target e' by not exceeding a threshold ε for each training observation.

Eventually, the performance of employed trained-SVMs will be assessed using the testing subset. A vector H which belongs to the testing subset is concurrently fed to SVC and SVR, and the pertaining outputs O and O' are attained. The output vector O will contain a sole '+1' element and '−1s' elements elsewhere due to the binary classification tendency of SVC. As a result, the location of '+1' will refer to the determined modulation type. In addition, SVR will directly yield an output scalar O' which returns SNR estimate.

Both the determined and actual signal types and SNR values are compared, and determination accuracies are subsequently calculated. The entire simulation is iterated 50 times and the mean determination accuracies are obtained.

V. SIMULATION RESULTS

To validate the performance of the presented mechanism, various simulations have been conducted. A broad range of SNR values (71 values) is considered in the conducted simulations i.e., 0–35 dB with a step of 0.5 dB.

First, the relation between the selected R significant-PCs and parameter ∇ is demonstrated by the curve given in Fig. 5. The parameter ∇ in (23) increases proportionally according to the quantities of the R-selected PCs (more specifically to their pertaining eigenvalues as manifested in the aforementioned equation). In this figure, the criterion in (23) is satisfied

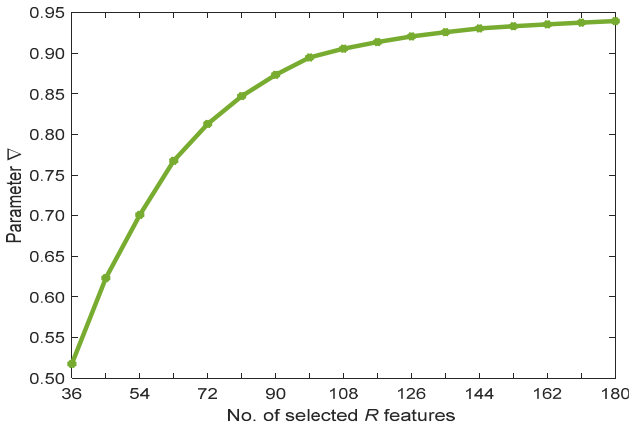

FIGURE 5. The relation between parameter ∇ and the selected R principal components PCs (features).

when minimum selected PCs is 12% of the entire features (i.e., 108 features). Consequently, it signifies the efficient exploitation of choosing a few PCs rather than processing the overall features. In fact, this essentially leads to less computational complexity and quicker processing for the presented determination mechanism.

Table 2 describes the identification accuracies for nine modulation types when exploiting the entire features. The overall identification accuracy for modulation recognition is determined by calculating the average of the nine individual recognition accuracies placed in the diagonal of Table 2 (shaded cells). The achievable overall identification accuracy of all modulation types is 99.06% notwithstanding the deterioration over the modulated signals caused by both AWGN and Rayleigh fading channels.

The effect of choosing a percentage of features on the overall modulation identification accuracy of the proposed scheme is portrayed in Fig. 6. It is evident from the figure that the determination accuracies exponentially improved with the increment of the chosen percentage of features. Furthermore, it is apparent that opting 8% of the entire number of features yields recognition accuracy approaching 70%. On the other hand, when considering 12% features

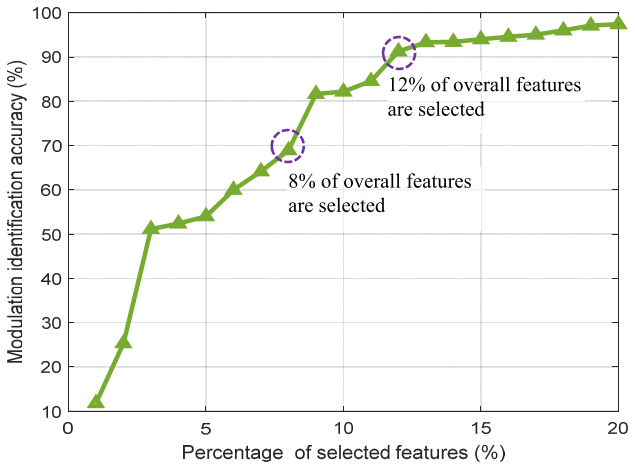

FIGURE 6. Effect of selected percentage of features (PCs) against the overall identification accuracy when splitting the dataset by 5-fold cross validation method.

and above, this accuracy attains values more than 91%. But, from 16% features selected onwards, the improvement of the recognition accuracies is slightly visible. It is notable to mention that all the aforementioned accuracy values have been achieved in the presence of AWGN and Rayleigh fading channels.

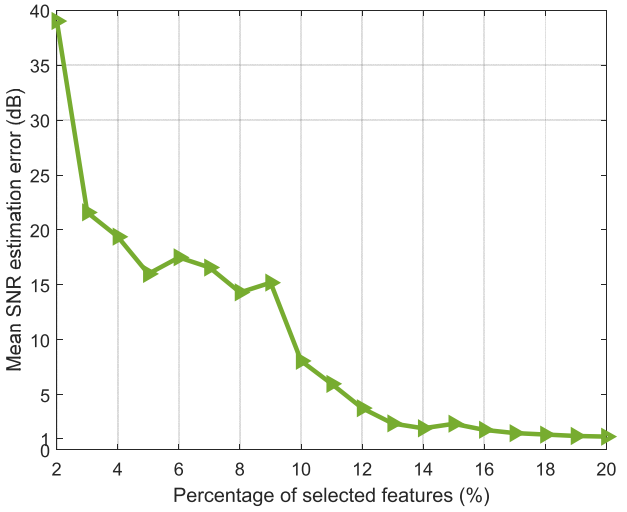

FIGURE 7. Mean estimation error of SNR as a function of the percentage of selected features.

On the other hand, the impact of tuning the percentage of optimum features on the mean SNR prediction error is manifested in Fig. 7. It is noticeably observed that selecting a higher percentage of optimum features leads to a proportional decrease in mean SNR estimation error. That is to say, when the percentage of chosen features rises, the mean prediction error of SNR declines, and conversely. Besides, when the percentage 16% (out of 900) of optimum features is considered, the resultant mean SNR prediction error is 1.81 dB. Furthermore, the mean prediction error values of SNR are 1.51 dB, 1.38 dB and 1.25 dB when the percentages of selected features are 17%, 18%, and 19% respectively. Additionally, selecting 20% of optimum features yields less than 1.2 dB average SNR estimation error. Nevertheless, the impact of increasing the percentage of chosen features on the decrement of SNR estimation error is slightly noticeable from 16% of selected features onwards. Table 3 numerically interprets the results illustrated in Fig. 6 and Fig. 7 for the determination of both modulation types and SNRs.

TABLE 3. Percentage of Features With Identification Accuracies and Regression Errors

Percentage of selected features (%)	Recognition accuracy % (modulation formats)	Mean Regression error dB (SNR)
2	25.34	39.01
3	51.13	21.59
4	52.39	19.38
5	54.02	16
6	59.98	17.51
7	64.16	16.58
8	68.92	14.32
9	82.17	15.20
10	81.64	8.08
11	84.58	5.99
12	91.26	3.78
13	93.32	2.39
14	93.40	1.95
15	94	2.36
16	94.57	1.81
17	95.04	1.51
18	95.99	1.38
19	97.09	1.25
20	97.41	1.19

As noticed in Table 3, considering a percentage of selected features of 16%, the determination values for both parameters (i.e. modulation type and SNR) are good. But going beyond 16%, the determination values approach a near plateau. This again demonstrates the advantage of exploiting PCA method to extract the most optimum features reflected by ASIQHs images, and to minimize their dimensions. Figure 8 portrays the outcomes of SNR predictions for nine signals namely BPSK, 2-ASK, 4-ASK, QPSK, 8-PSK, 4-QAM, 16-QAM, 32-QAM and 64-QAM using all features. Their individual mean SNR estimation errors are given in the Table 4.

TABLE 4. Mean SNR Estimation Errors and Their Corresponding Signals

Signal type	Mean Regression error (SNR)
BPSK	0.57
2-ASK	0.54
4-ASK	0.69
QPSK	0.58
8-PSK	0.68
4-QAM	0.63
16-QAM	0.76
32-QAM	1.23
64-QAM	4.28

As illustrated in Fig. 8, the presented scheme estimates the SNR with values quite close to the actual SNRs with an

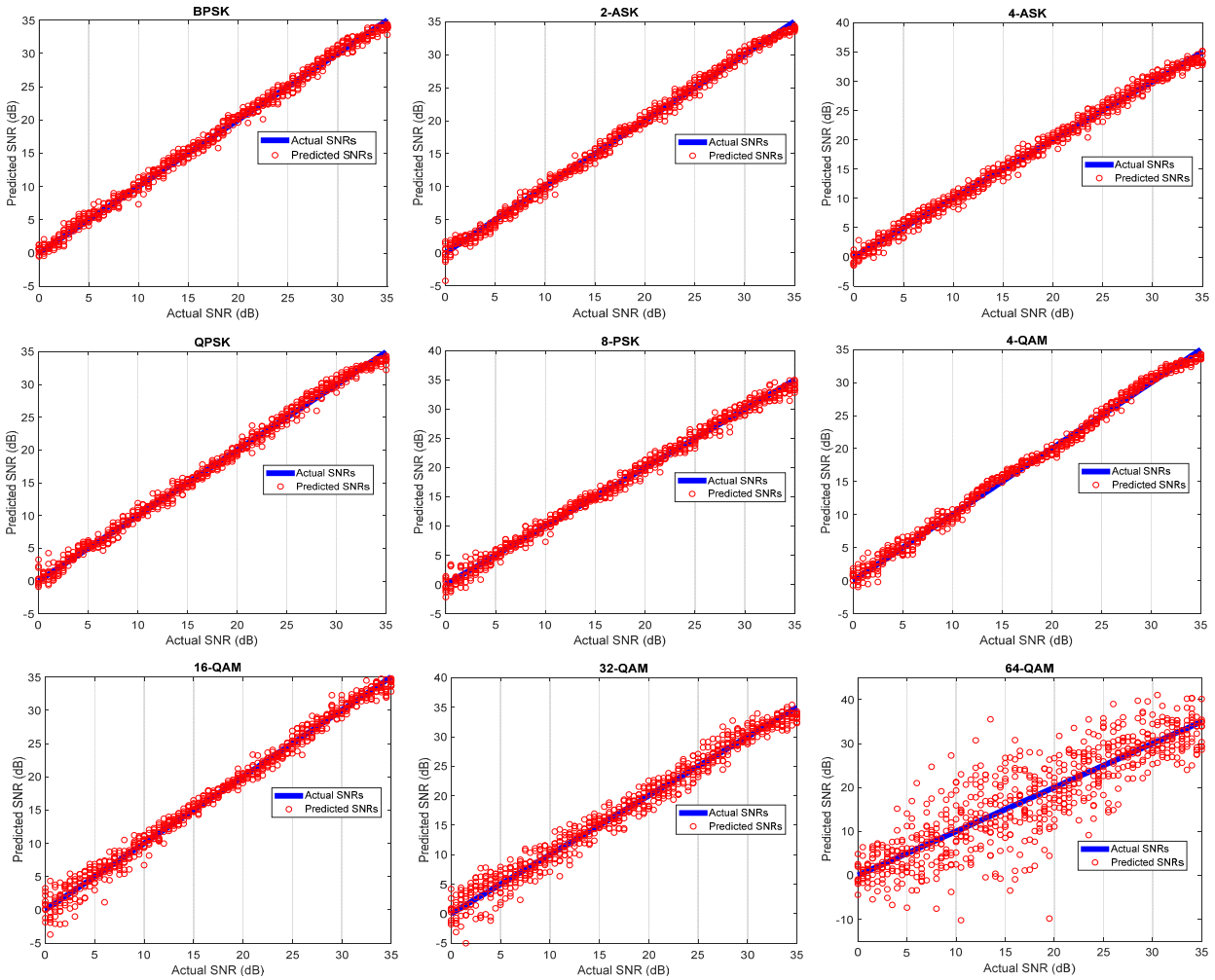

FIGURE 8. Actual versus estimated SNRs for BPSK, 2-ASK 4-ASK, QPSK, 8-PSK, 4-QAM, 16-QAM, 32-QAM, and 64-QAM signals using the proposed mechanism.

average estimation error 1.10 dB for all considered signals despite the deterioration effects of both Rayleigh fading and AWGN channels. However, from Fig. 8 and Table 4, when the modulation type 64-QAM is utilized to transmit the signal, the support vector regressor (SVR) in the receiver looks like experiencing some challenge to estimate the SNR of the transmitted 64-QAM-based signal.

This is mostly because of the extracted 64-QAM signatures nearly resemble each other at different SNR values, due to the severe Rayleigh fading impact as it can be observed in Fig. 9.

From Fig. 9 (a and b), the 64-QAM-based signatures (or the colored circles including the faded blue ones) show less sensitivity to the SNR variations as their patterns remain almost same. Thus, it becomes more challenging for the SVM to determine the SNR of the signal when high-order M-QAM (i.e. $M = 64$ and above) is used. Therefore, further enhancement of SNR estimation capabilities is required when advanced modulation schemes are utilized such as 64-QAM and beyond. Nevertheless, the density in pixels (i.e. the colored pixels including the faded blue ones) of these images is still slightly different. The sensitivity to SNR variations in these images gets much better after 3 dB onwards as the colored circles become slightly bigger and distinct from the signatures at 1 dB and 3 dB.

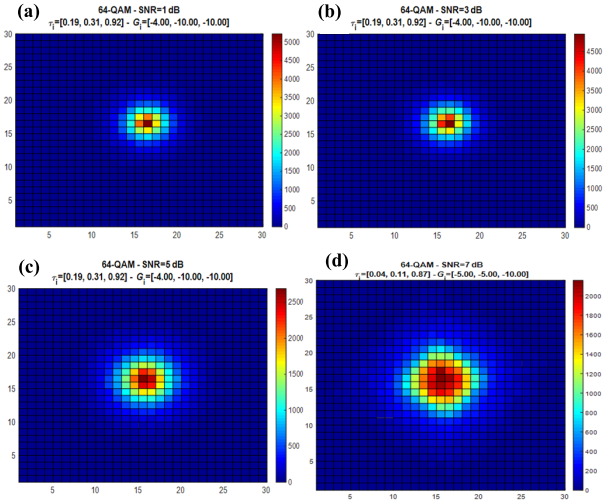

FIGURE 9. (64-QAM) signal at different low values of SNR, a) 64-QAM at $SNR = 1dB$, b) 64-QAM at $SNR = 3dB$, c) 64-QAM at $SNR = 5dB$, d) 64-QAM at $SNR = 7dB$, under Rayleigh fading channels.

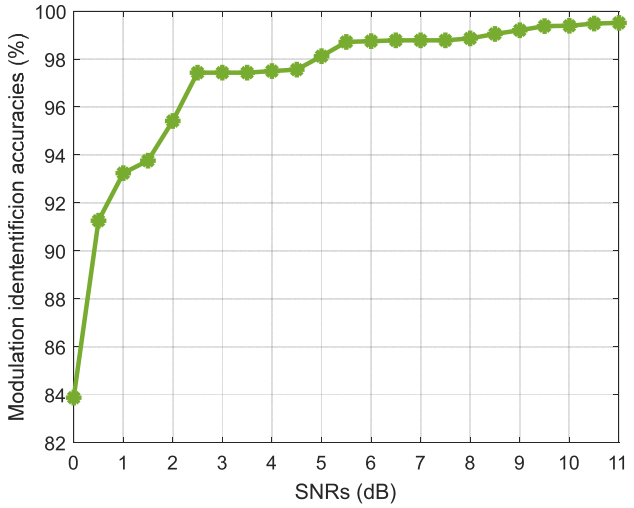

FIGURE 10. Modulation identification accuracies of the proposed scheme against SNRs in the presence of AWGN and Rayleigh fading channels.

Figure 10 reflects how the proposed scheme performs over different values of SNRs. It manifests that the recognition accuracies achieved good values even at low SNR ranges. For instance, it is almost 84% and higher than 93% at SNR values 0 dB and 1 dB respectively, while it is above 97% at SNR = 3 dB. From 5 dB onwards, the recognition accuracies remain high at 98% and above.

The results of joint classification and regression indicate the capability of the presented mechanism for simultaneous determination of modulation formats and SNRs and offer high accuracies despite the impact of AWGN and Rayleigh fading channels on the transmitted signals considered in this work. Credits are given to the robustness of the proposed 2D-ASIQHs features in combination with SVMs tool.

The proposed scheme provides simplicity in hardware implementation. That can be attributed to: 1) the simultaneous determination of multiple signal parameters which removed the necessity of utilizing a separate algorithm for every signal parameter, 2) the exploitation of ASIQHs which eliminates the need of timing knowledge as the scheme involves an asynchronous sampling process, 3) The scheme enables a generic receiver which is capable of detecting various signals impaired with multipath fading, an intelligent receiver that can estimate and track any fluctuations related to modulations and SNRs at the transmitter side and the channel, respectively, 4) simple structure of the receiver as the developed scheme exploited the existing structure of a coherent receiver circuit featuring built-in asynchronous low-speed samplers (i.e. sampling rate much less than symbol rate) without requiring any extra sampler components., 5) almost 85% reduction in the size of the utilized ASIQHs-based features using PCA method, which in practice leads to lowering the processing time, and computational and hardware complexity. Therefore, it is a promising low-cost alternative for several-parameters determination in future generations of wireless communication systems.

TABLE 5. A Comparison Between the Proposed Scheme and Existing Work

Reference	Channel effect	Recognized\estimated signal's parameters		Determination accuracies
		Modulation	SNR	
[53]	Flat fading	✓	×	98 %
[42]	Frequency selective fading	✓	×	93.21 %
[46]	AWGN	✓	✓	99.12 % , 0.88 dB
[27]	Flat fading	✓	×	98.25 %
[10]	AWGN	✓	×	97.74 %
[74]	AWGN	✓	×	95.40 % at SNR=−2dB
[36]	AWGN	✓	×	97 %
[44]	AWGN	×	✓	0.50 dB
The proposed work	AWGN and frequency selective fading (three paths)	✓	✓	99.06 %, 1.10 dB

Table 5 presents a compression between state-of-the-art related methods and the proposed scheme and highlights how the proposed work outperforms its peers despite the realistic impairments of frequency selective fading scenario.

VI. CONCLUSION

A novel scheme for simultaneous automatic determination of modulation types and SNR for 5G and beyond is proposed in this paper. The proposed mechanism is a new approach utilizing 2D-ASIQHs features to simultaneously recognize modulation types and estimate SNRs values by exploiting SVMs tool. In addition, the paper has proposed a scheme that enjoys a low implementation complexity. The scheme demonstrates robustness against AWGN and Rayleigh fading environments, attaining very good identification accuracy of 99.06% and reasonable mean estimation error of 1.10 dB for various modulation types and wide range of SNRs, respectively. Hence, the presented scheme can be an attractive and cost-effective option for future generations of wireless communication systems.

REFERENCES

[1] C.-X. Wang, F. Haider, X. Gao, X.-H. You, Y. Yang, D. Yuan, H. Aggoune, H. Haas, S. Fletcher, and E. Hepsaydir, "Cellular architecture and key technologies for 5G wireless communication networks," *IEEE Commun. Mag.*, vol. 52, no. 2, pp. 122–130, Feb. 2014.

[2] Z. Zhu and A. K. Nandi, *Automatic Modulation Classification: Principles, Algorithms and Applications*. Chichester, U.K.: Wiley, 2015.

[3] A. W. Azim, S. S. Khalid, and S. Abrar, "Non-data-aided SNR estimation method for APSK exploiting rank discrimination test," *Electron. Lett.*, vol. 48, no. 14, pp. 837–839, Jul. 2012.

[4] Y. A. Eldemerdash, O. A. Dobre, and M. Oner, "Signal identification for multiple-antenna wireless systems: Achievements and challenges," *IEEE Commun. Surveys Tuts.*, vol. 18, no. 3, pp. 1524–1551, 3rd Quart., 2016.

[5] O. Dobre, "Signal identification for emerging intelligent radios: Classical problems and new challenges," *IEEE Instrum. Meas. Mag.*, vol. 18, no. 2, pp. 11–18, Apr. 2015.

[6] M. Zhang, M. Diao, and L. Guo, "Convolutional neural networks for automatic cognitive radio waveform recognition," *IEEE Access*, vol. 5, pp. 11074–11082, 2017.

[7] F. N. Khan, C. Lu, and A. P. T. Lau, "Joint modulation format/bit-rate classification and signal-to-noise ratio estimation in multipath fading channels using deep machine learning," *Electron. Lett.*, vol. 52, no. 14, pp. 1272–1274, Jul. 2016.

[8] J. J. Popoola and R. van Olst, "The performance evaluation of a spectrum sensing implementation using an automatic modulation classification detection method with a universal software radio peripheral," *Expert Syst. Appl.*, vol. 40, no. 6, pp. 2165–2173, May 2013.

[9] E. Avci and D. Avci, "Using combination of support vector machines for automatic analog modulation recognition," *Expert Syst. Appl.*, vol. 36, no. 2, pp. 3956–3964, Mar. 2009.

[10] A. E. Sherme, "A novel method for automatic modulation recognition," *Appl. Soft Comput.*, vol. 12, no. 1, pp. 453–461, Jan. 2012.

[11] M. L. D. Wong and A. K. Nandi, "Automatic digital modulation recognition using artificial neural network and genetic algorithm," *Signal Process.*, vol. 84, no. 2, pp. 351–365, Feb. 2004.

[12] S. Norouzi, A. Jamshidi, and A. R. Zolghadrasli, "Adaptive modulation recognition based on the evolutionary algorithms," *Appl. Soft Comput.*, vol. 43, pp. 312–319, Jun. 2016.

[13] A. Ebrahimzadeh and S. E. Mousavi, "Classification of communications signals using an advanced technique," *Appl. Soft Comput.*, vol. 11, no. 1, pp. 428–435, Jan. 2011.

[14] Z. Wu, S. Zhou, Z. Yin, B. Ma, and Z. Yang, "Robust automatic modulation classification under varying noise conditions," *IEEE Access*, vol. 5, pp. 19733–19741, 2017.

[15] A. Serbes, H. Cukur, and K. Qaraqe, "Probabilities of false alarm and detection for the first-order cyclostationarity test: Application to modulation classification," *IEEE Commun. Lett.*, vol. 24, no. 1, pp. 57–61, Jan. 2020.

[16] Z. Xing and Y. Gao, "A modulation classification algorithm for multipath signals based on cepstrum," *IEEE Trans. Instrum. Meas.*, vol. 69, no. 7, pp. 4742–4752, Jul. 2020.

[17] M.-J. Hao, W.-L. Tsai, and Y.-C. Tsai, "Squared envelope-based SNR estimation," *J. Chin. Inst. Eng.*, vol. 36, no. 6, pp. 810–818, Sep. 2013.

[18] F.-X. Socheleau, A. Aissa-El-Bey, and S. Houcke, "Non data-aided SNR estimation of OFDM signals," *IEEE Commun. Lett.*, vol. 12, no. 11, pp. 813–815, Nov. 2008.

[19] S. D. Krishnamurthy and S. L. Sabat, "Blind SNR estimation for M-ARY frequency shift keying signal using covariance technique," *AEU Int. J. Electron. Commun.*, vol. 70, no. 10, pp. 1388–1394, Oct. 2016.

[20] D. R. Pauluzzi and N. C. Beaulieu, "A comparison of SNR estimation techniques for the AWGN channel," *IEEE Trans. Commun.*, vol. 48, no. 10, pp. 1681–1691, Oct. 2000.

[21] O. A. Dobre, A. Abdi, Y. Bar-Ness, and W. Su, "Survey of automatic modulation classification techniques: Classical approaches and new trends," *IET Commun.*, vol. 1, no. 2, pp. 137–156, Apr. 2007.

[22] J. Zheng and Y. Lv, "Likelihood-based automatic modulation classification in OFDM with index modulation," *IEEE Trans. Veh. Technol.*, vol. 67, no. 9, pp. 8192–8204, Sep. 2018.

[23] J. L. Xu, W. Su, and M. Zhou, "Software-defined radio equipped with rapid modulation recognition," *IEEE Trans. Veh. Technol.*, vol. 59, no. 4, pp. 1659–1667, May 2010.

[24] J. L. Xu, W. Su, and M. Zhou, "Likelihood-ratio approaches to automatic modulation classification," *IEEE Trans. Syst., Man, Cybern. C, Appl. Rev.*, vol. 41, no. 4, pp. 455–469, Jul. 2011.

[25] S. Huang, Y. Yao, Z. Wei, Z. Feng, and P. Zhang, "Automatic modulation classification of overlapped sources using multiple cumulants," *IEEE Trans. Veh. Technol.*, vol. 66, no. 7, pp. 6089–6101, Jul. 2017.

[26] H. Yu, L. Shi, Y. Qian, F. Shu, J. Li, Y. Zhao, and D. N. K. Jayakody, "A cooperative modulation recognition: New paradigm for power line networks in smart grid," *Phys. Commun.*, vol. 25, pp. 268–276, Dec. 2017.

[27] H. Tayakout, I. Dayoub, K. Ghanem, and H. Bousbia-Salah, "Automatic modulation classification for D-STBC cooperative relaying networks," *IEEE Wireless Commun. Lett.*, vol. 7, no. 5, pp. 780–783, Oct. 2018.

[28] Y. A. Eldemerdash and O. A. Dobre, "On the identification of SM and alamouti-coded SC-FDMA signals: A statistical-based approach," *IEEE Trans. Veh. Technol.*, vol. 65, no. 12, pp. 10079–10084, Dec. 2016.

[29] A. Swami and B. M. Sadler, "Hierarchical digital modulation classification using cumulants," *IEEE Trans. Commun.*, vol. 48, no. 3, pp. 416–429, Mar. 2000.

[30] M. Abdelbar, W. H. Tranter, and T. Bose, "Cooperative cumulants-based modulation classification in distributed networks," *IEEE Trans. Cognit. Commun. Netw.*, vol. 4, no. 3, pp. 446–461, Sep. 2018.

[31] A. Tsakmalis, S. Chatzinotas, and B. Ottersten, "Modulation and coding classification for adaptive power control in 5G cognitive communications," in *Proc. IEEE 15th Int. Workshop Signal Process. Adv. Wireless Commun. (SPAWC)*, Jun. 2014, pp. 234–238.

[32] E. E. Azzouz and A. K. Nandi, "Automatic modulation recognition-I," *J. Franklin Inst.*, vol. 334, no. 2, pp. 241–273, Mar. 1997.

[33] H.-C. Wu, M. Saquib, and Z. Yun, "Novel automatic modulation classification using cumulant features for communications via multipath channels," *IEEE Trans. Wireless Commun.*, vol. 7, no. 8, pp. 3098–3105, Aug. 2008.

[34] L. Yang, Z. Ji, X. Xu, X. Dai, and P. Xu, "Modulation classification in multipath fading environments," in *Proc. 4th Int. Symp. Wireless Commun. Syst.*, Oct. 2007, pp. 171–174.

[35] M. H. Shah and X. Dang, "Novel feature selection method using bhattacharyya distance for neural networks based automatic modulation classification," *IEEE Signal Process. Lett.*, vol. 27, pp. 106–110, 2020.

[36] X. Zhang, J. Sun, and X. Zhang, "Automatic modulation classification based on novel feature extraction algorithms," *IEEE Access*, vol. 8, pp. 16362–16371, 2020.

[37] X. Yan, G. Zhang, and H.-C. Wu, "A novel automatic modulation classifier using graph-based constellation analysis for M-ary QAM," *IEEE Commun. Lett.*, vol. 23, no. 2, pp. 298–301, Feb. 2019.

[38] M. A. Pinto-Orellana and H. L. Hammer, "Dyadic aggregated autoregressive model (DASAR) for automatic modulation classification," *IEEE Access*, vol. 8, pp. 156096–156103, 2020.

[39] S.-H. Kim, J.-W. Kim, V.-S. Doan, and D.-S. Kim, "Lightweight deep learning model for automatic modulation classification in cognitive radio networks," *IEEE Access*, vol. 8, pp. 197532–197541, 2020.

[40] E. Avci, D. Hanbay, and A. Varol, "An expert discrete wavelet adaptive network based fuzzy inference system for digital modulation recognition," *Expert Syst. Appl.*, vol. 33, no. 3, pp. 582–589, Oct. 2007.

[41] M. Türk and H. Oğraş, "Classification of chaos-based digital modulation techniques using wavelet neural networks and performance comparison of wavelet families," *Expert Syst. Appl.*, vol. 38, no. 3, pp. 2557–2565, Mar. 2011.

[42] M. H. Shah and X. Dang, "Robust approach for AMC in frequency selective fading scenarios using unsupervised sparse-autoencoder-based deep neural network," *IET Commun.*, vol. 13, no. 4, pp. 423–432, Mar. 2019. [Online]. Available: https://digital-library.theiet.org/content/journals/10.1049/iet-com.2018.5688

[43] T. A. Almohamad, M. F. M. Salleh, M. N. Mahmud, A. H. Y. Sa'd, and S. A. Al-Gailani, *Automatic Modulation Recognition in Wireless Communication Systems Using Feature-Based Approach*. Singapore: Springer, 2019, pp. 403–409.

[44] Y. Li, R. Liu, and R. Wang, "A low-complexity SNR estimation algorithm based on frozen bits of polar codes," *IEEE Commun. Lett.*, vol. 20, no. 12, pp. 2354–2357, Dec. 2016.

[45] T. A. Almohamad, M. F. M. Salleh, M. N. Mahmud, and A. H. Y. Sa'd, "Simultaneous determination of modulation types and signal-to-noise ratios using feature-based approach," *IEEE Access*, vol. 6, pp. 9262–9271, 2018.

[46] F. N. Khan, C. H. Teow, S. G. Kiu, M. C. Tan, Y. Zhou, W. H. Al-Arashi, A. P. T. Lau, and C. Lu, "Automatic modulation format/bit-rate classification and signal-to-noise ratio estimation using asynchronous delay-tap sampling," *Comput. Electr. Eng.*, vol. 47, pp. 126–133, Oct. 2015.

[47] F. N. Khan, Z. Dong, C. Lu, and A. P. T. Lau, "Optical performance monitoring for fiber-optic communication networks," in *Enabling Technologies for High Spectral-efficiency Coherent Optical Communication Networks* (Wiley Series in Microwave and Optical Engineering), X. Zhou and C. Xie, Eds. Hoboken, NJ, USA: Wiley, 2016.
[48] M. Bkassiny, Y. Li, and S. K. Jayaweera, "A survey on machine-learning techniques in cognitive radios," *IEEE Commun. Surveys Tuts.*, vol. 15, no. 3, pp. 1136–1159, 3rd Quart., 2013.
[49] C. Jiang, H. Zhang, Y. Ren, Z. Han, K.-C. Chen, and L. Hanzo, "Machine learning paradigms for next-generation wireless networks," *IEEE Wireless Commun.*, vol. 24, no. 2, pp. 98–105, Apr. 2017.
[50] R. Singh and S. Kansal, "Artificial neural network based spectrum recognition in cognitive radio," in *Proc. IEEE Students' Conf. Electr., Electron. Comput. Sci. (SCEECS)*, Mar. 2016, pp. 1–6.
[51] N. Kim, N. Kehtarnavaz, M. B. Yeary, and S. Thornton, "DSP-based hierarchical neural network modulation signal classification," *IEEE Trans. Neural Netw.*, vol. 14, no. 5, pp. 1065–1071, Sep. 2003.
[52] S. Kharbech, I. Dayoub, M. Zwingelstein-Colin, and E. P. Simon, "On classifiers for blind feature-based automatic modulation classification over multiple-input–multiple-output channels," *IET Commun.*, vol. 10, no. 7, pp. 790–795, May 2016.
[53] A. Ali and F. Yangyu, "Automatic modulation classification using deep learning based on sparse autoencoders with nonnegativity constraints," *IEEE Signal Process. Lett.*, vol. 24, no. 11, pp. 1626–1630, Nov. 2017.
[54] S. Rajendran, W. Meert, D. Giustiniano, V. Lenders, and S. Pollin, "Deep learning models for wireless signal classification with distributed low-cost spectrum sensors," *IEEE Trans. Cognit. Commun. Netw.*, vol. 4, no. 3, pp. 433–445, Sep. 2018.
[55] F. Meng, P. Chen, L. Wu, and X. Wang, "Automatic modulation classification: A deep learning enabled approach," *IEEE Trans. Veh. Technol.*, vol. 67, no. 11, pp. 10760–10772, Nov. 2018.
[56] M. Kulin, T. Kazaz, I. Moerman, and E. De Poorter, "End-to-end learning from spectrum data: A deep learning approach for wireless signal identification in spectrum monitoring applications," *IEEE Access*, vol. 6, pp. 18484–18501, 2018.
[57] S. Duan, K. Chen, X. Yu, and M. Qian, "Automatic multicarrier waveform classification via PCA and convolutional neural networks," *IEEE Access*, vol. 6, pp. 51365–51373, 2018.
[58] R. Li, L. Li, S. Yang, and S. Li, "Robust automated VHF modulation recognition based on deep convolutional neural networks," *IEEE Commun. Lett.*, vol. 22, no. 5, pp. 946–949, May 2018.
[59] R. Lin, W. Ren, X. Sun, Z. Yang, and K. Fu, "A hybrid neural network for fast automatic modulation classification," *IEEE Access*, vol. 8, pp. 130314–130322, 2020.
[60] F. Wang, S. Huang, H. Wang, and C. Yang, "Automatic modulation classification exploiting hybrid machine learning network," *Math. Problems Eng.*, vol. 2018, Dec. 2018, Art. no. 6152010.
[61] H. Hu, Y. Wang, and J. Song, "Signal classification based on spectral correlation analysis and SVM in cognitive radio," in *Proc. 22nd Int. Conf. Adv. Inf. Netw. Appl. (AINA)*, Mar. 2008, pp. 883–887.
[62] Y. Huang, H. Jiang, H. Hu, and Y. Yao, "Design of learning engine based on support vector machine in cognitive radio," in *Proc. Int. Conf. Comput. Intell. Softw. Eng.*, Dec. 2009, pp. 1–4.
[63] Y. Tan and J. Wang, "A support vector machine with a hybrid kernel and minimal vapnik-chervonenkis dimension," *IEEE Trans. Knowl. Data Eng.*, vol. 16, no. 4, pp. 385–395, Apr. 2004.
[64] J. Fan, J. Wang, and D. Zhao, *PolSAR Image Segmentation Based on the Modified Non-Negative Matrix Factorization and Support Vector Machine*. Cham, Switzerland: Springer, 2014, pp. 594–601.
[65] W. Kim, J. Park, J. Yoo, H. J. Kim, and C. G. Park, "Target localization using ensemble support vector regression in wireless sensor networks," *IEEE Trans. Cybern.*, vol. 43, no. 4, pp. 1189–1198, Aug. 2013.
[66] V. N. Vapnik, *The Nature of Statistical Learning Theory*. New York, NY, USA: Springer, 1995, p. 188.
[67] P. Liu, K.-K.-R. Choo, L. Wang, and F. Huang, "SVM or deep learning? A comparative study on remote sensing image classification," *Soft Comput.*, vol. 21, no. 23, pp. 7053–7065, Dec. 2017.
[68] J. K. Y. S. Cho, W. Y. Yang, and C. G. Kang, *MIMO-OFDM Wireless Communications With MATLAB*. Singapore: Wiley, 2010.
[69] D. W. G. James, T. Hastie, and R. Tibshirani, *An Introduction to Statistical Learning*. New York, NY, USA : Springer, 2013.
[70] X. Kong, C. Hu, and Z. Duan, *Principal Component Analysis Networks and Algorithms*. Singapore: Springer, 2017.
[71] I. T. Jolliffe and J. Cadima, "Principal component analysis: A review and recent developments," *Phil. Trans. Roy. Soc. A, Math., Phys. Eng. Sci.*, vol. 374, no. 2065, Apr. 2016, Art. no. 20150202.
[72] I. T. Jolliffe, *Principal Component Analysis* (Springer Series in Statistics), 2nd ed. New York, NY, USA: Springer-Verlag, 2002, p. 488.
[73] J. E. Jackson, *A User's Guide To Principal Components (Wiley Series in Probability and Statistics)*. Hoboken, NJ, USA: Wiley, 2004, p. 587.
[74] K. Zhang, L. Xu, Z. Feng, and P. Zhang, "A novel automatic modulation classification method based on dictionary learning," *China Commun.*, vol. 16, no. 1, pp. 176–192, 2019.

TARIK ADNAN ALMOHAMAD (Member, IEEE) received the B.Sc. degree in information engineering from the Department of Telecommunication Engineering, Ittihad Private University, Syria, in 2008, with two distinguished awards as top two performers, and the M.Sc. degree in electronic systems design engineering from USM, where he graduated as top-ranked. He worked as a Teaching Assistant and a Lab Demonstrator with Ittihad Private University from 2008 to 2010, and later joined the wireless cooperative communication projects at Universiti Sains Malaysia (USM), Nibong Tebal, Malaysia, as a Research Assistant. He is currently an Assistant Professor at the Electrical-Electronics Engineering Department, Faculty of Engineering, Karabük University. He was a recipient of the USM Fellowship during his Ph.D. program in the field of wireless and mobile systems, where he investigated the identification of signal's parameters in wireless communication systems.

MOHD FADZLI MOHD SALLEH (Member, IEEE) was born in Bagan Serai, Perak, Malaysia. He received the B.S. degree in electrical engineering from Polytechnic University, Brooklyn, NY, USA, in 1995, the M.S. degree in communication engineering from the University of Manchester Institute of Science and Technology (UMIST), Manchester, U.K., in 2002, and the Ph.D. degree from the University of Strathclyde, Glasgow, U.K., in 2006. Until July 2001, he was a Software Engineer with the Research and Development Department, Motorola Penang. He is currently an Associate Professor with the School of Electrical and Electronic Engineering, Universiti Sains Malaysia. He has supervised 12 Ph.D. degree students to graduation. His research interests include source coding and signal processing for application in telecommunications and wireless communication networks.

MOHD NAZRI MAHMUD received the B.Eng. degree in electronic systems engineering (telecommunications) from the Department of Electronic Systems Engineering, University of Essex, U.K., in 1996, and the M.Phil. degree in technology policy and the Ph.D. degree from the University of Cambridge, U.K., in 2003 and 2017, respectively. From 1996 to 2006, he was with Telekom Malaysia. Since 2006, he has been a Lecturer with the School of Electrical and Electronic Engineering, Universiti Sains Malaysia.

İSMAIL RAKIP KARAŞ received the B.Sc. degree from the Geomatics Engineering Department, Selcuk University, in 1997, the M.Sc. degree from the Geomatics Engineering Department, Gebze Institute of Technology, in 2001, and the Ph.D. degree from the GIS and Remote Sensing Program, Geomatics Engineering Department, Yildiz Technical University, in 2007. In 2002, he involved in a GIS project at the Forest Engineering Department, Oregon State University, USA. During the various periods of 2010, 2011, and 2014, he was a Visiting Researcher with the 3D GIS Research Lab, Faculty of Geoinformation Science and Engineering, Universiti Teknologi Malaysia. From 2000 to 2009, he was a Research Assistant with the Geomatics Engineering Department, Gebze Institute of Technology. Since 2009, he has been with Karabük University, Turkey, and taught undergraduate and graduate classes in geoinformation and computer sciences. He is currently a Professor of the Computer Engineering Department and also the Head of the 3D-GeoInformatics Research Group, Karabük University, where he is also the Dean of the Safranbolu Fine Art and Design Faculty. He has involved in Tubitak, EU, and other national and international projects and got various awards and supports during his research activities. He is on the Editorial Board of the *International Journal of Geo-Spatial Knowledge and Intelligence*, the *American Journal of Geographic Information System*, and some others.

NOR SHAHIDA MOHD SHAH (Member, IEEE) received the B.E. degree in electrical and electronic from the Tokyo Institute of Technology, Japan, in 2000, the master's degree in optical communication from the University of Malaya, Malaysia, in 2003, and the Ph.D. degree in electrical, electronics and system engineering from Osaka University, Japan, in 2012. She is currently a Senior Lecturer with Universiti Tun Hussein Onn Malaysia. Her research interest includes optical and wireless communication.

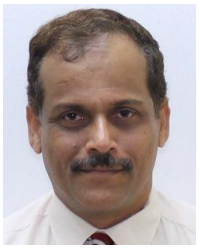

SAMIR AHMED AL-GAILANI (Member, IEEE) received the B.Sc. degree from Aden Yemen, in 1992, and the Ph.D. degree in optoelectronics from Universiti Technologi Malaysia (UTM), in 2014, with Best Student Award. He started his career as a Senior Lecturer with the Higher Technical Institute. Since 2014, he has been given various responsibilities including teaching, postdoctoral fellow, supervising laboratory sessions, supervising post-graduate students and undergraduate students, academic advisor, head of laboratory, head of research group, chairman and member of different committees, conducting short courses and training. He has authored 20 ISI articles. He has an H-Index of seven and total citations of 212, presented more than 90 articles in reputed refereed conferences. He also successfully supervised nine undergraduate students.